AD_____

Award Number: DAMD17-99-1-9239

TITLE: Prediction of Pathologic Fracture Risk in Activities of Daily Living and Rehabilitation of Patients with Metastatic Breast Carcinoma of the Pelvis and Femur

PRINCIPAL INVESTIGATOR: Nozomu Inoue, M.D., Ph.D.

CONTRACTING ORGANIZATION: The Johns Hopkins University
School of Medicine
Baltimore, Maryland 21205-2196

REPORT DATE: August 2000

TYPE OF REPORT: Annual

PREPARED FOR: U.S. Army Medical Research and Materiel Command
Fort Detrick, Maryland 21702-5012

REPORT DOCUMENTATION PAGE

Form Approved
OMB No. 074-0188

1. AGENCY USE ONLY (Leave blank)	2. REPORT DATE	3. REPORT TYPE AND DATES COVERED
	August 2000	Annual (15 Jul 99 - 14 Jul 00)

4. TITLE AND SUBTITLE
Prediction of Pathologic Fracture Risk in Activities of Daily Living and Rehabilitation of Patients with Metastatic Breast Carcinoma of the Pelvis and Femur

5. FUNDING NUMBERS
DAMD17-99-1-9239

6. AUTHOR(S)
Nozomu Inoue, M.D., Ph.D.

7. PERFORMING ORGANIZATION NAME(S) AND ADDRESS(ES)
The Johns Hopkins University School of Medicine
Baltimore, Maryland 21205-2196

E-MAIL:
ninoue@jhmi.edu

8. PERFORMING ORGANIZATION REPORT NUMBER

9. SPONSORING / MONITORING AGENCY NAME(S) AND ADDRESS(ES)
U.S. Army Medical Research and Materiel Command
Fort Detrick, Maryland 21702-5012

10. SPONSORING / MONITORING AGENCY REPORT NUMBER

11. SUPPLEMENTARY NOTES
Report contains color photos

12a. DISTRIBUTION / AVAILABILITY STATEMENT
Approved for public release; distribution unlimited

12b. DISTRIBUTION CODE

13. ABSTRACT *(Maximum 200 Words)*

The purpose of the project is to develop a computer model of the pelvis and proximal femur which can be used to predict the pathologic fracture risk and study the effects of pelvic and proximal femoral metastatic bone lesions on the care and management of breast cancer patients. The scope of the research is to construct graphical and quantitative models of the pelvis and proximal femur on computer workstations including Finite Element Method (FEM) and Discrete Element Method (DEM) to study the stress and strain in the pelvis and proximal femur and pressure distribution of the hip joint in the patient with metastatic bone lesions of the breast cancer in the pelvis and proximal femur with interactive capability. A database of the metastatic breast cancer to the pelvis and femur has been established for modeling the pelvis and femur with metastatic breast carcinoma. An interactive DEM model has been developed to calculate the pressure distribution of the hip joint with the bone defect. A pilot study of motion capture was performed to determine an appropriate system for acquisition of kinematic data in Activity in Daily Living, rehabilitation program, and nursing care for the metastatic breast cancer patients.

14. SUBJECT TERMS
Breast Cancer, Bone Metastasis, Pathological Fracture, Virtual Reality Computer Model, Rehabilitation and Nursing Care, QOL

15. NUMBER OF PAGES
15

16. PRICE CODE

17. SECURITY CLASSIFICATION OF REPORT	18. SECURITY CLASSIFICATION OF THIS PAGE	19. SECURITY CLASSIFICATION OF ABSTRACT	20. LIMITATION OF ABSTRACT
Unclassified	Unclassified	Unclassified	Unlimited

NSN 7540-01-280-5500

Standard Form 298 (Rev. 2-89)
Prescribed by ANSI Std. Z39-18
298-102

Table of Contents

INTRODUCTION

The subject of the project is to develop models to predict the pathological fracture risk in activities in daily living life, nursing care, and rehabilitation in breast cancer patients with metastatic lesion in the pelvis and proximal femur. The purpose of the project is to develop a computer model of the pelvis and proximal femur which can be used to predict the pathologic fracture risk and study the effects of pelvic and proximal femoral metastatic bone lesions on the care and management of breast cancer patients. The scope of the research is to include the construction of graphical and quantitative models of the pelvis and proximal femur on computer workstations including Finite Element Method (FEM) and Discrete Element Method (DEM) to study the stress/strain in the pelvis and proximal femur and pressure distribution of the hip joint in the patient with metastatic bone lesions of the breast cancer in the pelvis and proximal femur with interactive capability.

BODY

This section describes the research accomplishment associated with each Task outlined in the approved Statement of Work (written in italic letters).

Technical Objectives 1: Computer model construction

Task 1: Months 1-6: Establishment of database for location, size, and distribution of metastatic breast cancer to pelvic and femoral regions.

Seventy-three data sheets of the metastatic breast cancer to pelvis and femur were created including the radiographic analysis and a database was established (**Appendix 1** and **Table 1**). This geometrical data will be incorporated into FEM and DEM in the **Task 2**. In addition to the geometrical data, the distribution of the normal pressure on the hip joint during the normal activity will also be mapped to the three dimensional model (**Fig. 1**). This database also includes other information beside the location and the size of the metastatic lesion, such as period from the diagnosis of the breast carcinoma to the diagnosis of the bone lesion, pre-surgical function, histology of the metastatic lesion, type of surgery, and post-surgical function. This data could be used for evaluation of the QOL of the breast carcinoma patient with bone metastasis from multiple points of view.

Task 2: Months 6-18: Development of Multi-Discrete Element Model (DEM) and Finite Element Model (FEM) of pelvic and femoral regions based on the database established in Task 1.

An interactive DEM model of the hip joint has been developed (**Fig. 2**). This model allows creation of a bone metastasis induced defect at the hip joint surface of any size or location interactively. The model demonstrates the remarkable changes in the pressure distribution in the hip joint when the bone defect exists at the joint surface (**Fig. 3**). Because of the interactive capability, the DEM analysis of the hip joint could be performed on an individual basis. The DEM analysis on sacro-ilium (SI) and pubic-symphysis (PS) joints and FEM analysis in the pelvis and proximal femur will be performed in Year-2.

Task 3: Months 6-12: Mechanical testing using cadaveric specimens of pelvic region with and without bone defects in the pelvis.

The Dynamic Joint Simulator to be used for **Task 3**, which was located at our second Biomechanics Laboratory at the Good Samaritan Hospital, has been relocated to our main laboratory at

the Ross Research Building in May, 2000. This moving required disassembles and reassembles of the machine, minor renovation of the laboratory, tuning of the machine, and up-grading of the system. The final up-grading will be accomplished in late August, 2000. Even though this relocation caused a delay of **Task 3**, it will increase the efficacy of the experiment because the Good Samaritan Hospital is located 5 miles away from the Ross facility where all staff of the Biomechanics Lab stay. Another testing machine, MTS BIONIX 858, and peripheral equipment to be used for **Task 4** are also located at the Ross facility. Setting the Dynamic Joint Simulator and MTS BIONIX 858 testing machine side by side at the Ross facility allows more effective mechanical testing using cadaveric specimens of pelvis and proximal femur. The **Task 3** will be combined with **Task 4** and accomplished in the same period as the **Task 4**.

Task 4: Months 13-18: Mechanical testing using cadaveric specimens of pelvic region with and without bone defects in the proximal femur.

See a section of **Task 3**.

Technical Objectives 2: Establishment of the model to predict fracture risk in activities in daily living life, nursing care, and rehabilitation

Task 5: Months 19-22 Acquisition of kinematic and force data in Activity in Daily Living (ADL), rehabilitation program, and nursing care.

A pilot study of motion capture was performed using an optical motion tracking system to determine an appropriate marker placement for acquisition of kinematic data in Activity in Daily Living, rehabilitation program, and nursing care (**Fig. 4**).

The following tasks will be performed after Month 23 as planed.

Task 6: Months 23-28: Analysis of the loading conditions during the activities studied in Task 5.

Task 7: Months 29-33: Analysis of the stability and stress/strain distribution in the metastatic pelvis and proximal femur under the loading conditions predicted in Task 6.

Task 8: Months 34-36: Preparation of publications.

In addition to the approved Tasks, we performed quantitative analysis of the trabecular structure in the cortical defect healing. This data will be required to estimate mechanical properties of the healing bone defect caused by bone metastasis. This result has been presented at the Annual meeting of Orthopaedic Research Society, Orlando, 2000 (**Appendix 4**).

KEY RESEARCH ACCOMPLISHMENT

- The database of the metastatic breast cancer to pelvis and femur has been established.
- The basis of the new biomechanical model using DEM to estimate the pressure distribution of the hip joint with bone defect has been developed.
- The pilot study for acquisition of kinematic data in Activity in Daily Living (ADL), rehabilitation program, and nursing care has been initiated even though this task has been planed to start late half of Year-2.

REPORTABLE OUTCOMES

- Manuscripts, abstracts, presentations;

Manuscript: Outcomes of periacetabular osteotomy –Joint contact pressure calculation using standing AP radiographs- (in preparation)

Abstract: Rafiee B, Inoue N, Jones K, Deitz L, Aro H, Chao E: Trabecular microstructure in the early stage of cortical defect repair. Transaction of the 46th Annual Meeting of Orthopaedic Research Society. Vol. 25, 216, 2000, Orlando, March 12-15, 2000.

Presentation Chao E, Nobuhara K, Elias J, Inoue N, Mattessich S, Nakamura Y: Application of visual, interactive, computational models to orthopaedic surgery. 67th Annual Meeting of American Academy of Orthopaedic Surgeons. Orlando, March 15-19, 2000.

- Patents and licenses applied for and/or issued;

  None
- Degrees obtained that are supported by this award;

  None
- Development of cell lines, tissue or serum repositories;

  None
- Informatics such as databases and animal models, etc;

  1. The database for the metastatic breast cancer to pelvic and femoral regions
  2. Interactive Discrete Element Model to calculate pressure distribution at the surface of the hip joint with any defect (source code is written with C++ language)
- Funding applied for based on work supported by this award;

  None
- Employment or research opportunities applied for and/or received on experiences/training supported by this award.

  The Principal Investigator of this award, Nozomu Inoue, M.D., Ph.D., has been promoted to Associate Professor of Department of Orthopaedic Surgery, Johns Hopkins University in May, 2000.

  The Post-Doctoral fellow, Mehran Armand, Ph.D., funded by this award (50% of his time) has been promoted to Senior Professional Staff, Technical Service Department at Applied Physics Laboratory (APL), Johns Hopkins University in July, 2000. He worked on developing the Discrete Element Model of the hip joint in this project. Currently, he is working on a hip model to predict hip fracture caused by motor vehicle accident at APL based on his experiences/training supported by this award.

  A new Post-Doctoral fellow, Yoon Kim, Ph.D., has been recruited from Korea for the replacement of Dr. Armand in Feburuary, 2000. All materials related to this project have been transferred from Dr. Armand to Dr. Kim during the last 5 months.

CONCLUSIONS

The database of the metastatic breast cancer to pelvis and femur has been established for the creation of pelvic and femoral models with metastatic breast carcinoma. This database could also be used for other purposes such as evaluation of the QOL of the breast carcinoma patient with bone metastasis.

The newly developed interactive DEM model used to estimate the pressure distribution of the hip joint with bone defect is a key part of the model development in the awarded project. This model could also be applied to degenerative diseases of the hip joint and in intra-articulator fracture cases.

In order to perform the Tasks planned in Year 2-3 in this award, the pilot study of motion capture was performed to determine an appropriate system setting for acquisition of kinematic data in Activity in Daily Living, rehabilitation program, and nursing care.

REFERENCES

(1) Refereed Journal Articles

Meffert RH, Inoue N, Tis JE, Brug E, Chao EY: Distraction osteogenesis after acute limb-shortening for segmental tibial defects. Comparison of a monofocal and a bifocal technique in rabbits. J Bone Joint Surg Am. 2000 ;82(6):799-808.

Cooper RA, Quatrano LA, Axelson PW, Harlan W, Stineman M, Franklin B, Krause JS, Bach J, Chambers H, Chao EY, Alexander M, Painter P: Research on physical activity and health among people with disabilities: a consensus statement. J Rehabil Res Dev. 1999 ;36(2):142-54. Review.

Lietman SA, Inoue N, Chao EY, Frassica FJ: Distal femoral osteoarticular allografts in limb salvage surgery. Ann Chir Gynaecol. 1999;88(3):221-5.

Riley LH 3rd, Frassica DA, Kostuik JP, Frassica FJ: Metastatic disease to the spine: diagnosis and treatment. Instr Course Lect. 2000;49:471-7.

Frassica FJ, Frassica DA, McCarthy EF, Riley LH 3rd: Metastatic bone disease: evaluation, clinicopathologic features, biopsy, fracture risk, nonsurgical treatment, and supportive management. Instr Course Lect. 2000;49:453-9.

Virolainen P, Inoue N, Nagao M, Ohnishi I, Frassica FJ, Chao EY: Autogenous onlay grafting for enhancement of extracortical tissue formation over porous-coated segmental replacement prostheses. J Bone Joint Surg Am. 1999 ;81(4):493-9.

Nelson JB, Nguyen SH, Wu-Wong JR, Opgenorth TJ, Dixon DB, Chung LW, Inoue N: New bone formation in an osteoblastic tumor model is increased by endothelin-1 overexpression and decreased by endothelin A receptor blockade. Urology. 1999 ;53(5):1063-9.

(2) Abstracts

Rafiee B, Inoue N, Jones K, Deitz L, Aro H, Chao E: Trabecular microstructure in the early stage of cortical defect repair. Transaction of the 46th Annual Meeting of Orthopaedic Research Society. Vol. 25, 216, 2000, Orlando, March 12-15, 2000.

(3) Book Chapter

Chao EY, Inoue N, Elias JJ, Frassica FJ: Image-based computational biomechanics of the musculoskeletal system. In: Bankman, ed. *Handbook of Medical Imaging.* The Netherlands: Academic Press, (in press)

Appendix 1

RETROSPECTIVE REVIEW FORM OF METASTATIC BREAST CARCINOMA TO PELVIS AND FEMUR

1. Age of breast carcinoma diagnosis

2. Period from breast carcinoma diagnosis to metastatic bone lesion discovery

3. Period from metastatic bone lesion discovery to fracture

4. Type of fracture:
   - 1 = impending
   - 2 = active

5. Period from metastatic bone lesion discovery to diagnosis of bone lesion

6. Single or multiple bone fracture

7. Primary tumor histology

8. Grade of histological malignancy

9. Weight (kg) of the patient at fracture

10. Functional status (prefracture):
    - 1 = ambulatory without aids
    - 2 = ambulatory with aids
    - 3 = mobilized in a wheelchair
    - 4 = bedridden
    - 5 = unknown

11. Other coexisting disease

12. Other site of metastasis

13. Preoperative pain status:
    - 1 = at the lesion of metastasis
    - 2 = adjacent joint
    - 3 = other site
    - 4 = none

14. Condition of the primary lesion:
    - 1 = completely cured
    - 2 = suspicious residual tumor
    - 3 = obvious residual tumor
    - 4 = untreated
    - 5 = unknown

<u>Radiographic analysis at first fracture</u>

15. Location in the bone:
    - 1 = epiphysis
    - 2 = epiphysis - methaphysis
    - 3 = methaphysis
    - 4 = methapysis - diaphysis

5 = diaphysis, proximal third
6 = diaphysis, mid third
7 = diaphysis, distal third
8 = sacrum
9 = ilium
10 = ischium
11 = pubis
12 = acetablum

16. X-ray report: 1 = soft tissue mass, 2 = no mass

17. Tumor manifestation:
1 = osteoblastic
2 = osteolytic
3 = mixed

Size of bone lesion

18. Dimension AP:
1 = <50% of bone diameter
2 = 50< , <75%
3 = 75< , <100%
4 = unmeasurable

19. Dimension Lateral:
1 = <50% of bone diameter
2 = 50< , <75%
3 = 75< , <100%
4 = unmeasurable

Primary treatment of metastatic bony lesion

20. Radiation:
1= none
2 = before surgery
3 = after surgery
4 = before and after

21. Chemotherapy: 1 = no, 2 = yes

22. Other nonoperative treatment: 1 = no, 2 = yes

Surgical treatment:

23. Period from diagnosis of bone lesion to surgery

24. Type of surgery:
1 = no surgery
2 = no removal of the tumor
3 = biopsy alone
4 = curettage
5 = resection, not curative
6 = resection, curative
7 = amputation
8 = others

25. Tissue diagnosis

26. Materials used at the surgery

Post-surgical rehabilitation

27. Period from the surgery to rehabilitation

28. Period from the surgery to first walk after surgery with any aid

29. Period from the diagnosis of bone lesion to last follow-up or death

30. Status at the last follow-up:
    1 = alive with disease
    2 = alive without disease
    3 = alive unknown disease
    4 = dead with disease
    5 = dead without disease
    6 = dead unknown disease

31. Postoperative pain status:
    1= greatly relieved
    2 = slightly relieved
    3 = no change
    4 = worse
    5 = unknown

32. Best functional status after surgery:
    1 = ambulatory
    2 = ambulatory with aids
    3 = mobilization in a wheelchair
    4 = bedridden
    5 = unknown

33. Failure of treatment:
    1 = no failure
    2 = technical error in surgery
    3 = tumor progression
    4 = inadequate care after surgery
    5 = surgical complication
    6 = others

34. Progression locally: 1 = no, 2 = yes

35. Site of other pathologic fracture

36. Pattern of tumor invasion:
    1 = expensile
    2 = permiative
    3 = others

Appendix 2

Table 2 Retrospective Review of Metastatic Breast Carcinoma to Pelvis and Femur

(All female. Only items related to Task1 are shown.)

File #	Age at Dx (yrs)	Period from tumor Dx to bone metastasis discovery (months)	Impending/ Actual fracture I: Impending fracture F:Actual fracture	Functional status (pre-fracture) 1: ambulatory without aids 2: ambulatory with aids 3: mobilized in a wheel-chair 4: bedridden 5: unknown	Location of bone lesion 1: epiphysis 2: epiphysis - methaphysis 3 : methaphysis 4 : methapysis - diaphysis 5: diaphysis, proximal third 6 : diaphysis, mid third 7: diaphysis, distal third 8: sacrum 9: ilium 10: ischium 11: pubis 12: acetablum	Tumor manifestation 1: osteoblastic 2: osteolytic 3: mixed	Tumor size 1: <50% of bone diameter 2: 50<, <75% 3: 75<, <100% 4: unmeasurable		Surgery code 1: no surgery 2: no removal of the tumor 3: biopsy alone 4: curettage 5: resection, not curative 6: resection, curative 7: amputation 8: others
							AP	Lateral	
003	35	155	I	1	4	3	3	3	4
007	54	146	I	1	5	2	3	3	2
008	49	67	I	1	8	-	-	-	1
013	60	52	F	3	6	2	3	3	4
015	50	0	F	1	3	2	3	3	5
017	71	157	F	2	5	2	3	3	4
019	83	20	I	1	4	2	3	3	4
019B	83	20	I	1	8, 9	-	-	-	1
032	63	45	F	2	3	2	4	4	5
033B	75	98	I	2	6	3	4	4	2
033C	75	98	I	2	8	-	-	-	1
034	65	0	I	1	2	-	-	-	1
035	73	0	I	1	5	3	3	3	2
038	60	27	F	2	3	2	2	2	5
044	56	41	I	1	1	-	-	-	1
046	53	36	F	2	4	3	4	4	5
046B	53	36	I	2	8, 11	-	-	-	1
048	49	142	F	2	7	2	4	4	4
049	45	29	F	3	4	3	4	4	5
051	58	47	F	2	3	3	4	4	5
052	61	240	F	1	-	-	-	-	5
073	59	24	I	2	6	3	4	4	2
075	54	27	I	1	2	3	3	3	5
079	65	108	I	2	6	2	3	3	4
084B	47	0	I	1	4	2	3	-	2
086	47	20	F	1	1	2	2	2	5
089	44	135	I	2	6	2	2	2	2
089A	44	135	I	2	8	-	-	-	1
089B	44	144	I	2	6	2	4	4	2
090	45	37	I	1	2	2	3	-	5
090B	45	37	I	2	10, 12	-	-	-	1
092	45	57	I	2	3	2	3	-	5
092B	45	57	I	2	8	-	-	-	1
093	57	72	F	2	3	3	4	4	5
096	39	76	I	2	6	2	3	2	2

File #	Age at Dx (yrs)	Period from tumor Dx to bone metastasis discovery (months)	Impending/ Actual fracture I: Impending fracture F:Actual fracture	Functional status (pre-fracture) 1: ambulatory without aids 2: ambulatory with aids 3: mobilized in a wheel-chair 4: bedridden 5: unknown	Location of bone lesion 1: epiphysis 2: epiphysis - methaphysis 3 : methaphysis 4 : methapysis - diaphysis 5: diaphysis, proximal third 6 : diaphysis, mid third 7: diaphysis, distal third 8: sacrum 9: ilium 10: ischium 11: pubis 12: acetablum	Tumor manifestation 1: osteoblastic 2: osteolytic 3: mixed	Tumor size 1: <50% of bone diameter 2: 50<,<75% 3: 75<,<100% 4: unmeasurable		Surgery code 1: no surgery 2: no removal of the tumor 3: biopsy alone 4: curettage 5: resection, not curative 6: resection, curative 7: amputation 8: others
							AP	Lateral	
098A	53	39	I	1	5	2	3	3	4
098B	53	51	I	2	3	2	3	3	5
098C	53	51	I	2	8	-	-	-	1
103	37	5	F	1	3	2	4	4	5
109	47	13	I	1	6	2	4	2	4
113A	75	16	F	2	5	2	4	4	4
113B	75	21	F	2	2	2	4	4	5
223C	75	21	I	2	11	-	-	-	1
114A	38	84	F	2	3	2	4	4	5
114B	38	84	I	2	8	-	-	-	1
116A	55	103	F	2	3	2	4	4	5
116B	55	103	F	2	5	3	4	4	4
116C	55	103	I	2	10	-	-	-	1
117	65	24	F	2	5	2	4	4	2
117A	65	24	I	2	8	-	-	-	1
120	68	36	I	2	3	2	3	3	5
121	57	24	I	2	11	-	-	-	1
124B	56	112	I	2	4	2	4	4	2
126	24	2	I	2	2	2	4	4	5
127	53	17	I	2	4	2	3	-	4
132	37	74	I	2	5	2	4	4	2
137	41	55	F	1	3	3	4	4	5
141	50	142	I	2	3	3	4	4	5
142	51	34	I	1	5	2	4	4	4
143	56	89	I	2	6	3	4	4	2
146	45	13	I	2	-	-	-	-	5
150	29	15	F	2	5	2	3	3	4
155A	54	97	F	1	5	3	4	4	4
156	42	60	F	1	3	2	4	4	5
157	44	51	I	1	3	2	3	4	4
160A	43	131	F	1	3	2	4	4	4
161	58	89	F	1	3	2	4	4	5
162	41	58	I	1	5	2	4	4	2
177B	65	58	I	1	6	2	3	3	4
186	63	135	F	1	2	2	4	4	5
200	50	0	I	1	1	1.	1	1	1
201	26	168	I	1	2	2	1	-	1
203	55	24	I	1	12	3	4	-	1

Appendix 3

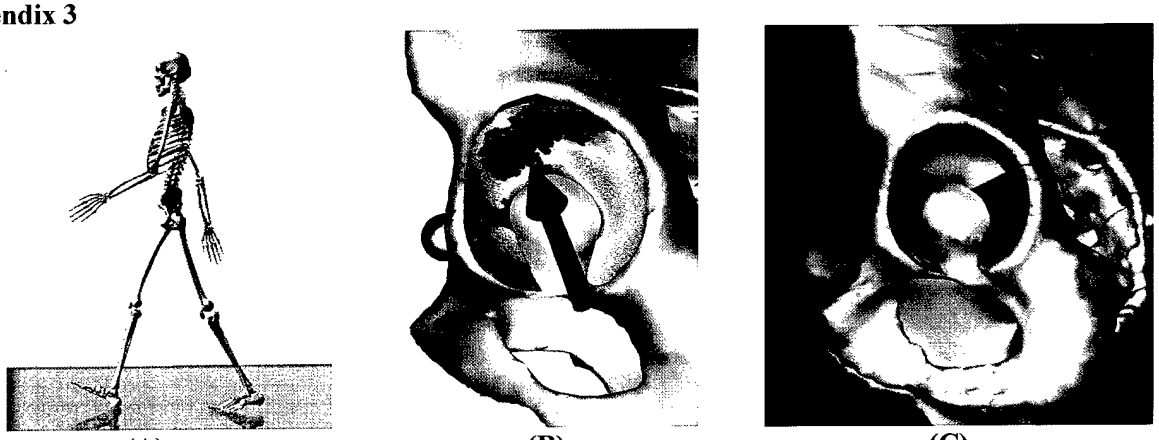

(A) (B) (C)

Figure 1 (A) Geometric model of skeleton shown at 55% gait cycle. **(B)** Acetabular pressure distribution with the force direction and magnitude represented by a vector. The darkest regions indicate the largest pressures. **(C)** The acetabular surface was divided into 4 regions based on the pressure distribution during the normal gait.

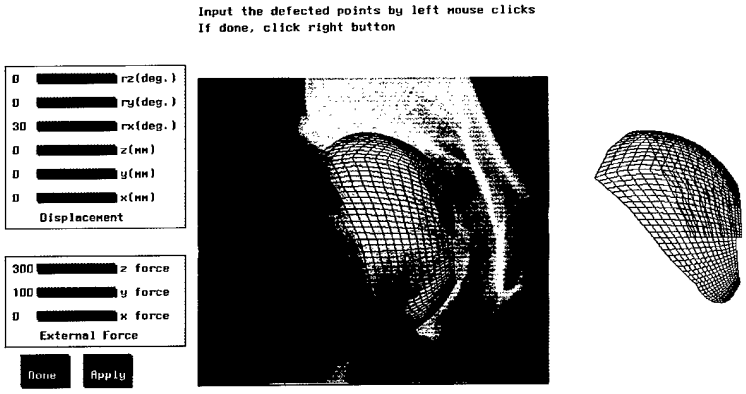

Figure 2 Interactive DEM model of the hip joint. Loading conditions and geometry of the acetablum can be input interactively (left and middle). The defect can be generated in any size and location on the surface of the contact surface of the hip joint (left) interactively as well.

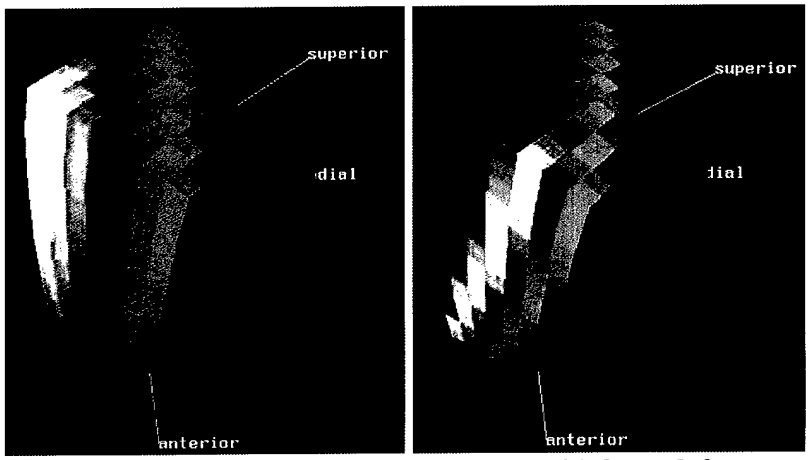

(A) Without bone defect **(B) With bone defect**

Figure 3 Pressure distribution of the hip joint without **(A)** and with **(B)** bone defect calculated by DEM. In this example, the contact pressure is distributed evenly in the loading area and the peak pressure is 5.6 MPa **(A)**. Remarkable increase of pressure is calculated in the adjacent area of the defect (peak pressure is 10.3 MPa) **(B)**.

Appendix 4

TRABECULAR MICROSTRUCTURE IN THE EARLY STAGE OF CORTICAL DEFECT REPAIR

*Rafiee, B; *Inoue, N (A-Department of The Army); *Jones, K; *Deitz, L; *Aro, H; +*Chao, E
+*Orthopaedic Biomechanics Laboratory, Johns Hopkins University, Baltimore, Maryland. Ross Research Building, 720 Rutland Avenue, Room 235, Baltimore, MD 21205, 410-502-6416, Fax: 410-502-6414, eychao@eagle.gsh.jhu.edu

INTRODUCTION: Cortical bone defect repair contrasts fracture and osteotomy healing by its stable mechanical condition. Lacking a cartilaginous phase, it follows an intramembranous ossification[1] specifically termed "angiogenic ossification" by Krompecher[2]. The limited available studies on cortical defect repair have used small circular defects[1] which fail to create a sufficient stress-strain gradient to fully characterize the influence of mechanical loading on the repair process. This study quantitatively analyzed trabecular orientation in a rectangular, high stress-strain gradient, cortical defect during its early stage of repair.

METHODS: Rectangular bone defects of dimensions 0.25 OD (the outer diameter of the tibia) by 1.5 OD (approximately, 2.5x15 mm) were created in the mid-diaphysis of the medial cortex of the right tibia in seven beagles by drilling 2.4 mm holes and connecting them with a fine osteotome. Dogs were euthanized after 4 weeks of unrestricted weight bearing. The proximal half of the defect was cut into six 1 mm thick transverse sections, processed undecalcified, and embedded in MMA (Fig. 1). The 2nd, 4th, and 6th sections were ground to 100 μm. The 1st, 3rd, and 5th transverse sections were each further cut longitudinally in the medial tibial plane, parallel to the defect surface, to form four 100 μm thick longitudinal sections, three from the defect area and one from anterior portion of the medullary canal (Fig. 1). Contact microradiographs of the transverse and longitudinal sections were made and digitized under 50x light microscopy for 2-dimensional Fast Fourier Transform (FFT) analysis. Transverse section images were divided into 9 fields in the defect area and 15 in the medullary canal (Fig. 3). Longitudinal sections of the defect area and medullary canal were divided into 3 and 5 fields, respectively. Each field corresponded to a 0.85 mm x 0.85 mm area in the radiograph and a 256x256 pixel array in the digitized image. FFT yielded a quantified orientation angle and intensity for each field (Fig. 2D-F). Statistical significance of the variance in angle and intensity of orientations in the above mentioned fields was demonstrated by ANOVA with corroborating post-hoc t-tests.

RESULTS: No clear bone formation was observed from the periosteal surface. Generally, repair bone trabeculae oriented from the medullary canal towards the bone defect. The intensity of trabecular orientation was higher in the defect area than in the medullary canal ($p<0.01$). These intradefect trabeculae oriented parallel to the defect walls. The vectorial mean angles of trabecular orientation in the fields chosen in the edge transverse sections had statistically significant differences from those in the center section ($p<0.05$). Analysis of the longitudinal sections quantified that trabeculae in the middle of the defect, on the outermost surface, were oriented along the longitudinal axis of the bone, but this orientation changed to a transverse direction in the deeper layers. In the longitudinal sections, the first two layers of the center field demonstrated statistically significant differences in the angle of orientation from fields to either side and in deeper layers ($p< 0.05$).

DISCUSSION: Early in the repair phase of a round cortical defect in rabbits, Shapiro proposed a rich vascular ingrowth from the medullary canal towards the defect, perpendicular to the cortical haversian systems, followed by woven bone and trabecular formation parallel to this vascular pattern[1]. Suwa used the microvascular casting method to analyze microvascular and trabecular changes in defect repair and demonstrated similar results[3]. Highly oriented trabecular structure in the defect area may reflect the structure of early vascular networks. Redirection of trabecular structure towards the osteonal direction was not observed by Shapiro's model even 12 weeks after surgery. In the current study, trabecular orientation in the osteonal direction was observed in a limited area. This may be caused by a higher stress-strain gradient around the bone defect[4]. Some trabecular orientation initiated from the endosteal surface adjacent to the defect towards the defect was observed in transverse section 6, from near the edge of the defect. It may be related to the higher stress-strain gradient in the corresponding area. Recent studies indicate the presence of growth factors and cytokines which may induce angiogenesis within the cortex and molecular transport through load-induced fluid flow[5-8]. Further study will be required to elucidate the contribution of the existing cortical bone to the defect healing process.

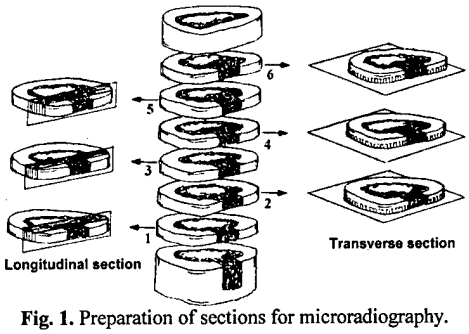

Fig. 1. Preparation of sections for microradiography.

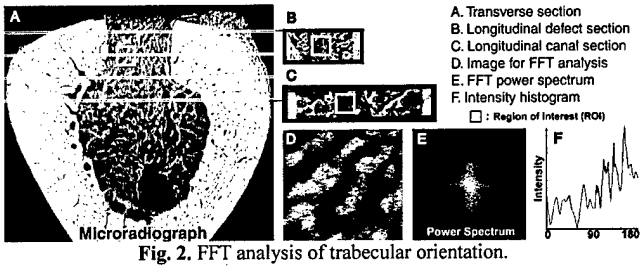

Fig. 2. FFT analysis of trabecular orientation.

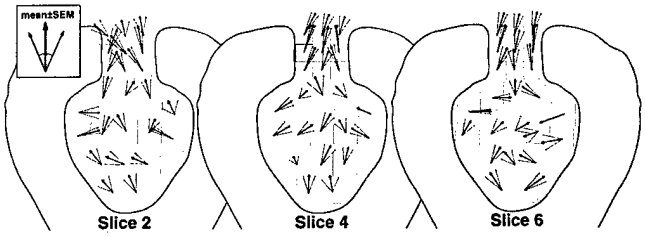

Fig. 3. Results of mean angle and intensity of the trabecular orientation.

REFERENCES: 1)Shapiro F:JBJS 70A,1067-81,1988. 2)Krompecher S: Verhand Anat Gesellshaft 42,34-53,1934. 3)Suwa F et al:J Osaka Dent Univ 32, 27-34,1998. 4)Elias J et al: Trans ORS23,973,1998. 5)Dekel S et al: JBJS 63B,185-9,1981. 6)Harada S et al:CORR313,76-80,1995. 7)Murry D & Rushton N:Calcif Tissue Int47,35-9,1990. 8)Knothe Tate M et al:Bone 22, 107-17,1998.